1-1-2012

Polymer chain distribution reorganization for improving the power conversion efficiency of polymer solar cells

Baofu Ding

Kamal Alameh
Edith Cowan University

POLYMER-CHAIN-DISTRIBUTION REORGANIZATION FOR IMPROVING THE POWER CONVERSION EFFICIENCY OF POLYMER SOLAR CELLS

BAO-FU DING AND KAMAL ALAMEH

Electron Science Research Institute, Edith Cowan University, 270 Joondalup Dr, Joondalup, WA 6027, Australia
E-mail: b.ding@ecu.edu.au; k.alameh@ecu.edu.au

ABSTRACT

We investigate the influence of the post solvent evaporation time delay on the performance of polymer solar cell (PSC) devices employing a bulk heterojunction photoactive polymer layer of regioregular poly(3-hexylthiophene) as electron donor and polymer [6,6]-thienylC61 butyric acid methyl ester as an electron acceptor. Characterization of the fabricated solar cell devices clearly demonstrates balanced transport of electrons and holes in the blend and confirms increased surface roughness and crystallinity of the films when post solvent evaporation time delay is optimised. An optimum device performance is obtained with 72 hours of post solvent evaporation time delay, achieving a power conversion efficiency of 4.1%, which is 0.9% higher than similar devices made without enough time for polymer-chain-distribution reorganization.

INTRODUCTION

The power conversion efficiencies of thin-film polymer solar cells (PSCs) have significantly increased over the last decade, mainly through the combination of new organic materials and enhanced device structures. While the power conversion efficiency (PCE) of these thin-film

V. Rajendran, P. Paramasivam and K.E. Geckeler (eds.)
Advanced Nano Materials for Industrial Applications, pp. 261-268 (2012).

organic solar cells is still lower than that attained by their inorganic counterparts, the attractive features of low cost, simple fabrication and wide choice of materials have been the driving force for the wide acceptance and commercialization of PSCs for the Green Energy market [1,2].

The improvement of the PCE of PSCs has recently become a challenging research area [3-5]. Among the many approaches used for improving the PCE of PSCs, the widely adopted one is based on solvent annealing after blending and spin-coating the polymer layers [1,6].

With the use of a sufficient self-organization time after annealing, the mobilities of electron and hole can be made more balanced, resulting in negligible carrier accumulation, and thus, high PSC performance.

In this paper, we propose a new approach based on introducing an additional (Step III) annealing time for polymer-chain-distribution reorganization (PCDR), which enables a higher PCE to be attained, in comparison with conventional two-step solvent annealing processes.

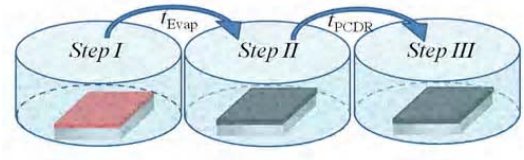

Fig. 1: Processing Steps for the Development of Polymer Solar Cells (i) Fresh Spin Coating of Blended Polymers, (ii) Phase Separation, After Solvent Evaporation Time, (iii) Proposed Additional Annealing time for PCDR

EXPERIMENT

Figure 1 shows the proposed processing steps for the development of polymer solar cells, namely (i) fresh spin coating of blended polymers, (ii) phase separation, achieved by evaporating solvent at room temperature for around 20 mins, and (iii) additional annealing time for tens of hours in order to reorganize the polymer chain distribution, and hence increase exciton dissociation, leading to a higher PCE.

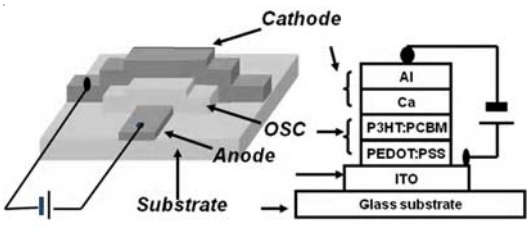

Fig. 2: Schematic View and Architecture of the PSC

The developed PSC structure is shown in Fig. 2. It comprised the following layers: (i) ITO, (ii) Poly(3,4-ethylenedioxythiophene) poly(styrenesulfonate) (PEDOT: PSS) (42 nm),

(iii) Poly(3-hexylthiophene) (P3HT): phenyl C61 butyric acid methyl ester (PCBM) (205 nm), (iv) Ca(20nm) and (v) Al (90nm). The ITO-coated glass substrate, which had a sheet resistance of 22 ohm, were cleaned as described in Ref. [7]. A thin layer (~30 nm) of PEDOT/PSS (Baytron P VP A1 4083) was spin-coated at a spinning speed of 3500 rpm for 40 seconds to make the ITO surface smoother and increase its work function. The ITO/PEDOT/PSS substrate was backed at 130 °C for 15 mins, and then transferred to a nitrogen-filled glove box (O_2<1 p.p.m. and H_2O<1 p.p.m.) for further processing. P3HT was first dissolved in 1,2-dichlorobenzene (DCB) to make 18 mg/ml solution, which was then blended with PCBM in 50 wt% and stirred for ~18 h at 35°C. Subsequently, the three processing steps shown in Fig. 1 were carried out, namely:

I. 60 µ the solution was spin coated on the PEDOT:PSS-coated substrate with a spinning speed of 700 rpm for 30 s to form the active layer of the PSC. The thickness of this active layer was around 190 nm as measured with a profiler.

II. The sample was put into a special Petri dish of 2.5 cm diameter and 1.5 cm height for solvent evaporation [1]. The evaporation time, t_{Evap}, is the time needed to change color of the top film from red to black.

III. The sample remained in the same Petri dish for PCDR for a time t_{PCDR}.

After the above three steps, the sample was thermal annealed, using a hot plate, at 120ºC for 15 minutes. Finally, Ca and Al layers were thermally evaporated at 0.8Å/s and 1.4Å/s, respectively, in a vacuum chamber at a pressure of 6×10^{-6} Pa to form a composite cathode of Ca(20nm)/Al(90nm). The top Al layer crossed the bottom ITO to form active device area of approximately 1.5 mm^2. Five similar PCDR devices were fabricated and processed with different polymer-chain-distribution reorganization times, namely, t_{PCDR} = 0 h, 24 h, 48 h, 72 h and 240 h, and their performances were experimentally evaluated.

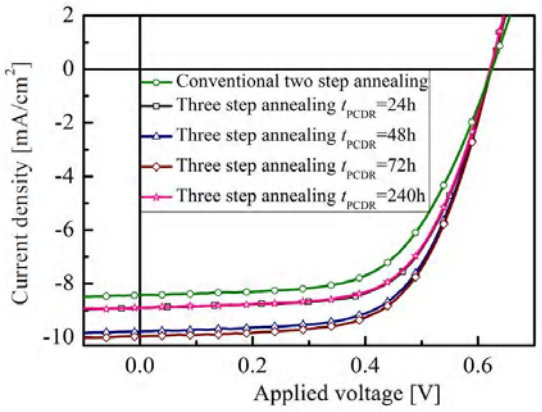

Fig. 3: Current Density Versus Applied Voltage for Different t_{PCDR}. Illumination = 1 sun. t_{PCDR} = 0 Corresponds to a Conventional two-step Process

Table 1: Summary of Device Performance for Various PV Devices in the Work

t_{PCDR} (h)	J_{sc} (mA/cm^2)	FF (%)	V_{oc} (V)	PCE (%)
0	8.4	60.0	0.63	3.2
24	8.9	64.3	0.62	3.5
48	9.8	63.6	0.62	3.9
72	10.2	63.6	0.62	4.1
240	8.9	63.5	0.62	3.6

RESULTS AND DISCUSSION

The current density versus voltage characteristics of the various PSCs fabricated with different t_{PCDR} are shown in Fig. 3 and summarized in Table 1. It is obvious that PSC that was post processed with t_{PCDR} = 72 h displays the best performance. Compared to a conventional PSC fabricated with a two-step process, the short circuit current (J_{sc}) and PCE of the PSC post processed with t_{PCDR} = 72 h increase from 8.4 mA/cm^2, 3.3% to 10.2 mA/cm^2, 4.1% at t_{PCDR} = 72 h. Noticeably, the fill factor (FF) increases from 60% (t_{PCDR} = 0 h) to 64.3% (t_{PCDR} = 24 h), then stays almost the same as t_{PCDR} increases.

For the improvement of FF, charge balance plays a key role. When the charge transport for electrons and holes in the device is unbalanced, the accumulation of majority carriers in the bulk of the polymer layer results in the space-charge-limited current. In this case, the photocurrent is governed by a square-root dependence on bias [8-10], and hence, FF will have a small value. Therefore, a balanced charge transport is the prerequisite to achieving a high FF. To measure the mobilities of electrons (μ_e) and holes (μ_h) for the PSCs, the space-charge-limited-current (SCLC) method was employed, which is comprehensively described in Refs [8,11]. An electron-dominant device of ITO/Ca/P3HT: PCBM/Ca/Al and a hole dominant device of ITO/PEDOT:PSS/P3HT:PCBM/Au were fabricated to measure μ_e and μ_h, respectively. For the electron-dominant device, the low work functions of Ca (2.8 eV) on both sides of the polymer P3HT:PCBM active layer make them efficient for injecting electrons and blocking holes into the polymer layer [12,13]. Therefore, the majority carries in the organic bulk are electrons. Oppositely, the high work functions of PEDOT:PSS (5.2eV) and Au (5.3 eV) favor hole injection from electrodes to the polymer layer [1,14], making holes the majority carriers for the latter device. By using the SCLC expression given in [8,11] *J-V* curves were generated for the above-described devices and fitted with experimentally measured curves, leading the evaluation if the electron and hole moblities μ_e and μ_h, which were 9.6×10^{-4} cm^2/Vs, 4.5×10^{-4} cm^2/Vs, respectively, for the two-step PSC device (t_{PCDR}=0 h) and 6.5×10^{-4} cm^2/Vs and 6.3×10^{-4} cm^2/Vs for the three-step optimized PSC device (t_{PCDR}=72 h). Here, the charge-balance ratio is defined as $\mu_e\mu_h$. For the two-step film, the ratio is around 2.1, which is similar to the value reported in [1]. On the other hand, for the 3-step PSC device, the ratio is significantly reduced to 1.03. Such a close-to-unity charge-balance ratio further improves the FF and results

in a higher PCE. Generally, the charge-balance ratio depends on the self-organization ability of the polymer chain. According to [1], the degree of self-organization is determined by t_{Evap}, which is the time needed for the wet films to solidify. After solidification, t_{PCDR} allows for the reorganization of polymer chain distribution as well as self-organization which can be monitored by measuring the surface roughness of the active layer [15].

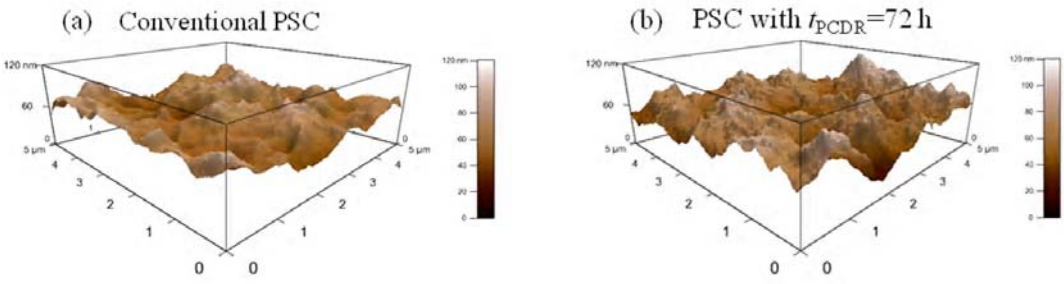

Fig. 4: Effects of t_{PCDR} on the Morphology of the Polymer Layer; AFM Height Images of the P3HT/PCBM Composite Films Showing a 5 μm → Á5 μm Surface Area. (a) Conventional PSC with t_{PCDR} =0 h, (b) PSC with t_{PCDR} =72 h

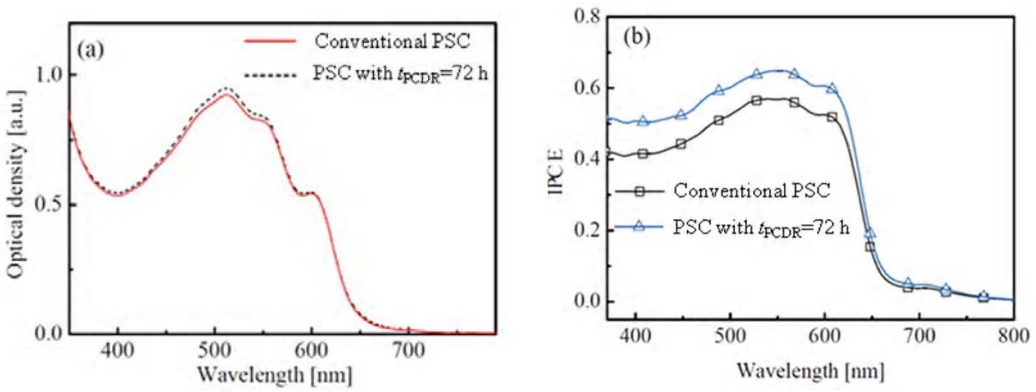

Fig. 5: Effects of t_{PCDR} on the (a) Absorbance of the P3HT/PCBM Films and (b) IPCE of the Conventional and Optimized PSC Devices

Figures 4(a) and 4(b) show atomic force microscopy (AFM) images of the conventional two-step PSC device and the optimized three-step PSC device, respectively, revealing three features that contribute to increasing the PSC performance: 1) For the two-step film, the surface is relative smooth, with an r.m.s. roughness of 9.9 nm (Fig. 4(a)). This result is in agreement with that reported by Li Gang et al. [1]. For the three-step film, a rougher surface is observed with roughness of 16.9 nm. This agrees with the earlier discussion that the extra time t_{PCDR} allows self-organization of the active layer leading to a higher surface roughness. 2) The

rougher morphology likely increases the contact area between the active layer and the cathode (Ca/Al composite), which enhances electron extraction to the cathode. 3) The peak-to-valley polymer height for the three-step PSC device is around 120 nm, corresponding to ~60% of the mean thickness, while the height is only 80 nm for the conventional two-step PSC device. Such large peak-to-valley height effectively reduces the charge-transport distance and thus increases J_{sc}.

To examine whether the introduction of step III influences the composition of the polymer layer, the optical absorption spectra, which depend on the composition of the bulk polymer, were measured for both the conventional two-step PSC device and the optimized three-step PSC device. As shown in Fig. 5(a), almost no change is observed in the absorption spectra, which implies that the thickness and composition of the film are not altered during step III. On the other hand, the internal photon-to-charge efficiency (IPCE) shown in Fig. 5(b) obviously increases after step III. Generally, the enhancement of absorption by the active layer is crucial to increase the IPCE. Figure 5(a) demonstrates that the composition of the active layer is insensitive to step III.

Thus the enhancement in absorption is due to the surface roughness of the active layer as confirmed by Figs. 4(a) and 4(b). To measure the absorption spectra, new two-step and three-step PSC devices were fabricated with the Ca/Al composite metal layer removed so that the devices were transparent. However, IPCE measurements were performed on PSC devices with highly reflective Ca/Al composite metal layers.

As seen in Figs. 4(a) and 4(b), the rougher surface of the active layer can scatter the incident light at the interface between the polymer layer and the cathode back into the active layer leading to enhanced absorption and increase in IPCE.

CONCLUSIONS

We have proposed and investigated the influence of the post solvent evaporation time delay on the performance of polymer solar cell (PSC) devices fabricated using the composite polymer P3HT:PCBM as the active layer. Experimental results have demonstrated a charge-balance ratio close to unity through the use of three processing steps, namely spin coating, solvent evaporation and polymer-chain-distribution reorganization time delaying. An optimum device performance has been obtained with 72 hours of polymer-chain-distribution reorganization time delay, displaying a power conversion efficiency of 4.1%, which is 0.9% higher than that of conventional two-step PSC devices.

ACKNOWLEDGEMENTS

This research is supported by Edith Cowan University, the Department of Industry, Innovation, Science, Research and Tertiary Education, Australia.

REFERENCES

[1] Li, G., Shrotriya, V., Huang, J.S., Yao, Y. and Moriarty, T. et al., High-efficiency solution processable polymer photovoltaic cells by self-organization of polymer blends. *Nat. Mater*. 4, 864-868, 2005.

[2] Yu, G., Gao, J., Hummelen, J.C., Wudl, F. and Heeger, A.J., Polymer Photovoltaic Cells: Enhanced Efficiencies via a Network of Internal Donor-Acceptor Heterojunctions. *Science* 270, 1789-1791, 1995.

[3] Woo, C.H., Beaujuge, P.M., Holcombe, T.W., Lee, O.P. and Freìchet, J.M.J., Incorporation of Furan into Low Band-Gap Polymers for Efficient Solar Cells. *J. Am. Chem. Soc*. 132, 15547-15549, 2010.

[4] Kekuda, D., Lin, H.-S., Chyi Wu, M., Huang, J.-S., Ho, K.-C. et al., The effect of solvent induced crystallinity of polymer layer on poly(3-hexylthiophene)/C70 bilayer solar cells. *Sol. Energ. Mat. Sol.* C 95, 419-422, 2011.

[5] Price, S.C., Stuart, A.C., Yang, L., Zhou, H. and You, W., Fluorine Substituted Conjugated Polymer of Medium Band Gap Yields 7% Efficiency in Polymer"Fullerene Solar Cells. *J. Am. Chem. Soc.* 133, 4625-4631, 2011.

[6] Li, G., Yao, Y., Yang, H., Shrotriya, V., Yang, G. et al., "Solvent annealing" effect in polymer solar cells based on poly(3-hexylthiophene) and methanofullerenes. *Adv. Funct. Mater*. 17, 1636-1644, 2007.

[7] Ding, B.F., Zhan, Y.Q., Sun, Z.Y., Ding, X.M., Hou, X.Y. et al., Electroluminescence and magnetoresistance of the organic light-emitting diode with a $La_{0.7}Sr_{0.3}MnO_3$ anode. *Appl. Phys. Lett*. 93, 183307, 2008.

[8] Davids, P.S., Campbell, I.H. and Smith, D.L., Device model for single carrier organic diodes. *J. Appl. Phys. 82*, 6319-6325, 1997.

[9] Mihailetchi, V.D., Xie, H.X., de Boer, B., Koster, L.J.A. and Blom, P.W.M., Charge transport and photocurrent generation in poly (3-hexylthiophene): Methanofullerene bulk-heterojunction solar cells. *Adv. Funct. Mater*. 16, 699-708, 2006.

[10] Reid, O.G., Munechika, K. and Ginger, D.S., Space Charge Limited Current Measurements on Conjugated Polymer Films using Conductive Atomic Force Microscopy. *Nano Lett*. 8, 1602-1609, 2008.

[11] Mihailetchi, V.D., van Duren, J.K.J., Blom, P.W.M., Hummelen, J.C., Janssen, R.A.J. et al., Electron Transport in a Methanofullerene. *Adv. Funct. Mater*. 13, 43-46, 2003.

[12] Jiang, C.Y., Sun, X.W., Zhao, D.W., Kyaw, A.K.K. and Li, Y.N., Low work function metal modified ITO as cathode for inverted polymer solar cells. *Sol. Energ. Mat. Sol*. C 94, 1618-1621, 2010.

[13] Zhao, D.W., Liu, P., Sun, X.W., Tan, S.T. and Ke, L. et al., An inverted organic solar cell with an ultrathin Ca electron-transporting layer and MoO[sub 3] hole-transporting layer. *Appl. Phys. Lett.* 95, 153304-153303, 2009.

[14] Sun, Z., Ding, B., Wu, B., You, Y., Ding, X. et al., LiF Layer at the Interface of Au Cathode in Organic Light-Emitting Devices: A Nonchemical Induced Carrier Injection Enhancement. *J. Phys. Chem. C* 116, 2543-2547, 2011.

[15] Lei, B., Yao, Y., Kumar, A., Yang, Y. and Ozolins, V., Quantifying the relation between the morphology and performance of polymer solar cells using Monte Carlo simulations. *J. Appl. Phys.* 104, 024504-024506, 2008.